Some Observations on the Development of Deformation Substructure in Zone-Refined Iron

J. T. Michalak and L. J. Cuddy
Edgar C. Bain Laboratory for Fundamental Research
United States Steel Corporation Research Center
Monroeville, Pennsylvania

Abstract

The development of the deformation substructure of zone-refined iron is similar to that observed for less pure vacuum-melted iron. Qualitative differences with increased purity are noted and are associated with a decrease in the dislocation sources and the necessity for cross-slip. Evidence is presented to show that, in the purest iron investigated, dislocation movement in the foil prepared for transmission electron microscopy is quite unrestricted and that the observed structures may not be typical of the dislocation density and distribution in the bulk.

Introduction

The importance of the substructure developed during plastic deformation of a body-centered-cubic metal cannot be denied. Keh (1) and Keh and Weissmann (2) have established experimentally a direct correlation of the dislocation density and distribution with the flow behavior of iron at 25 and -78°C. The relation between deformation substructure and mechanical properties of tantalum (3) and niobium (4) will be presented later in this Symposium. The role of substructure in recovery and recrystallization of iron and silicon-iron has been discussed by Leslie et al (5), Hu (6), and Walter (7). Substructure effects on strain aging in body-centered-cubic metals have been reviewed by Keh and Leslie (8), and by Rosenfield and Owen (9). The relations between substructure and precipitation phenomena are reviewed in other presentations of this Symposium (4,10).

The subject of this paper is the development of substructure during plastic deformation. Keh and Weissmann (2) have summarized the studies on the deformation substructure in body-centered-cubic metals and concluded that the dislocation structures of all of those investigated, which included iron, molybdenum, tungsten, tantalum and niobium, were similar. Dislocations were kinked and nonuniformly distributed in the early stage of deformation. As the amount of deformation was increased the distribution became more nonuniform and a cell structure was developed. This sequence of events is shown in Fig. 1. The walls of the cells are tangles of dislocations. For iron, the dislocation density was found to increase linearly with strain, and at a constant strain, to be independent of the deformation temperature below the temperature of recovery. The dislocation distribution in iron, however, was found to be temperature dependent; the distribution was more uniform and the tendency to form cells was decreased as the temperature of deformation was lowered. Keh and Weissmann (2) also showed that the relation between the dislocation density and the flow stress of iron was:

$$\sigma_f = \sigma_o + 0.17\ Gb\sqrt{N_f} \qquad (1)$$

where σ_f is the flow stress, σ_o is the frictional stress, G is the shear modulus ($=7.8\times10^3 kg/mm^2$), b is the Burgers vector of the slip dislocation in iron ($=2.5$ Å), and N_f is the dislocation density in the tangled regions. The change of the dislocation distribution with temperature, that is, the change in density within the tangles, accounts for the difference in flow behavior at different temperatures. Finally, it was observed that the dislocation density was dependent on grain size; a fine-grained iron exhibits a higher density of dislocations than does a coarse-grained iron strained to the same extent.

Materials and Experimental Procedure

The zone-refined iron and Fe-Mn alloy that have been studied by the present authors are listed in Table I, together with the method of purification and the final grain size obtained after cold work and recrystallization. In Table II the nominal content of carbon, nitrogen, hydrogen and oxygen is given in parts per million. All the materials were deformed in tension in bulk form and then thinned by electrolytic polishing to a final thickness suitable for examination by transmission electron microscopy.

Results and Discussion

A. Stress-Strain Behavior

The stress-strain curves for the polycrystalline, high-purity irons at several temperatures are given in Figs. 2-4. The results of tests at 25°C shown in Fig. 2 indicate that for the same grain size, there is not much difference in the tensile deformation of two irons of different overall purity. Reference to Table I indicates that iron B-3 had ten zone-refining passes compared to iron B-13 which received only one pass. It would be expected that the B-3 iron is the purer material, and although mechanical tests at 25°C do not support this, other differences in the behavior of these two irons do suggest that iron B-3 has less overall impurity. In processing these irons to a fine-grained aggregate from the zone-refined condition it was found that, after the same conditions of cold-rolling, iron B-13 required a recrystallization anneal at 650°C to produce a completely recrystallized uniform grain size of 43μ whereas iron B-3 could be recrystallized in the same time to the same uniform grain size at 600°C. The effects of small amounts of impurities on the recrystallization of iron have been investigated (11-13), and it has been observed that the purer the iron the lower the recrystallization temperature. It would appear, then, that room temperature tensile tests are not a reliable basis for evaluating the purity of iron. The lower stress levels of iron S-1, which is the least pure material on the basis of method of purification, can be accounted for by the larger grains in this iron, compared to the other two.

It will be noted from Fig. 3 that at -78°C a rather pronounced yield point drop becomes evident and that the rate of strain-hardening has decreased compared to room temperature tests. The pronounced yield point of the irons is a manifestation of an increased binding between interstitial atoms and potential dislocation sources as a result of a decrease in temperature. The increased yield point drop is not associated with a tearing away of dislocations from impurity atmospheres of increased binding, but rather with the decrease in the number of active sources of dislocations resulting from the increased binding. Keh and Weissmann (2) have suggested that the change in strain-hardening behavior with a change in temperature is associated with differences in the dislocation distribution during deformation at different temperatures. Although the average dislocation density is independent of test temperature, the dislocation distribution becomes more uniform as the temperature is decreased. Since the rate of work-hardening depends on

the density of dislocations within the tangled regions of the cell walls the more uniform distribution of dislocations results in a decreased rate of work hardening. The lower stress level and lack of a Lüders extension for iron S-1 is most probably a result of the larger grain size of this material.

The results of a temperature change during tests for iron B-3 are also shown in Fig. 3. They are consistent with the interpretation of Keh (1). He proposed that if a nonuniform distribution of dislocations is established by deformation at some temperature, then on subsequent testing at a lower temperature, characterized by a more uniform distribution, the flow stress at the lower temperature is greater than it would be if the specimen were strained to the same extent at the lower temperature only. The curvature of the stress-strain curve at the beginning of deformation at -78°C, after a prestrain at 25°C, makes it difficult to establish a well-defined initial flow stress at -78°C, but as can be seen, the flow stress at increasing strain rises above that for deformation only at -78°C, and the difference increases slightly with increased amount of prestrain at 25°C. As will be noted later, a strain of 3.75% at 25°C does not develop a gross nonuniform distribution of dislocations so that only a small difference in flow stress might be expected on subsequent straining at -78°C. Straining 7.5% at 25°C does develop some cell structure and a more nonuniform distribution so that continued deformation at -78°C results in the observed increase in flow stress.

Iron B-3 was the only high-purity iron which exhibited any plastic deformation at -196°C, and the results of testing at this temperature are shown in Fig. 4. Irons B-13 and S-1 failed predominantly by intergranular fracture at -196°C at stress levels of about 45-55 kg/mm^2.

Curve A in Fig. 4 represents the stress-strain behavior of iron B-3 deformed only at -196°C. Considerable twinning, as well as slip, was evident only during the Lüders extension. The Lüders extension in Fig. 4 is shown as a smooth line only for convenience. Fig. 5 is a light micrograph from a specimen, strained at -196°C, in which the Lüders front was allowed to pass through only about one-half of the gauge section. It is apparent from Fig. 3 and Fig. 4 that the rate of strain hardening, after the Lüders strain, is greater at -196°C than at -78°C, indicating a minimum in the temperature dependence of the rate of strain-hardening and a possible change in the mechanism of deformation at very low temperatures. A similar behavior has been observed by Keh and Weissmann (2).

Curves B, C and D of Fig. 4 are stress-strain curves at -196°C after a prestrain at 25°C of 0.75, 1.9 and 7.5% respectively. The prestrain at 25°C has eliminated completely the formation of twins at -196°C and, contrary to tests between 25 and -78°C, the flow stress at -196°C, after prestrain at 25°C, has not been increased above that for deformation only at -196°C. This observation also suggests a change in the mechanism of deformation as the temperature of deformation is decreased. This change in mechanism may be closely related to several observed factors: (a) the active

slip plane in iron becomes more restricted to the {110} planes (14) as the temperature is decreased; (b) the temperature dependence of the stress-velocity relationship for edge dislocations is greater for {112} planes than for {110} planes (15); (c) cross-slip of the screw dislocations becomes more difficult as the temperature is decreased (1,2).

B. Dislocation Sources

Before considering development of the deformation substructure it is necessary to establish what major source or sources of dislocations exist in the material prior to deformation. The sources of dislocations in any metal are: (a) random matrix dislocations, (b) the interfaces between the matrix and second-phase particles, (c) subboundaries within the grains, and (d) the grain boundaries. The random matrix dislocations which are not of the Frank-Read source type and which are not immobilized by impurity atmospheres will generate dislocations by the double cross slip mechanism (16), as has been shown by Low and Guard (17). The generation of dislocations at an inclusion-matrix interface under an applied stress has been reported (5,18). The formation of well-defined cell walls, after only light deformation, as a result of interaction of dislocations generated from closely spaced particles is illustrated in Fig. 6 from the work of Leslie, et al (5). Li (19) has considered the theoretical aspects of subboundary and grain boundary sources; Hornbogen (20) and Keh (1) have reported experimental evidence for subboundary and grain boundary sources. An example of dislocations originating from a grain boundary in an Fe-1.78 wt.% P alloy is shown in Fig. 7.

In fully recrystallized high-purity iron it has been observed that the number of second phase particles and subboundaries is so small as to be inconsequential as effective sources of dislocations. Likewise, the density of random dislocations, as measured by transmission electron microscopy and an X-ray technique discussed by Weissmann (21), is low and of the order of $10^6/cm^2$. Fig. 8 is a typical electron transmission micrograph of recrystallized high-purity iron illustrating this low dislocation density. Observations of dislocation loops emanating from grain boundaries (20), the "hairy" appearance of grain boundaries and the formation of irregular dislocation networks adjacent to the boundaries (1) after small deformations suggest that the grain boundaries and not the random matrix dislocations are the primary source of dislocations in high-purity iron. Li (19) has postulated that grain boundary ledges (or jogs) are the source of dislocations in the grain boundary. An example of the generation of a dislocation from a grain boundary ledge is shown in Fig. 9. The strain field of the ledge is shown only in one grain, although it could exist in both grains. It should be noted that this type of source is not a dislocation mill of the Frank-Read type which is capable of continuous generation. The grain boundary ledge is only a "donor" of dislocations and subsequent generation of dislocations within the grain can take place by the double cross-slip mechanism. According to Li's correlation between the density of grain boundary ledges and the Hall-Petch (22) slope, the decarburized Swedish iron studied by Codd and Petch (23) would have a ledge density of about 8×10^5 cm of ledge per cm^2 of grain boundary area. For a grain size of 100μ this would mean approximately 240 cm of ledge per grain, whereas the

nominal dislocation density within the grain of 10^6 cm/cm^3 provides about 0.5 cm of dislocation line within the grain. It is not unreasonable, then, that the primary source of dislocations is the ledges in the grain boundaries. Fig. 10 illustrates that ledges do in fact exist in the grain boundaries of a well annealed high-purity iron. The density of ledges in this micrograph is about 8×10^4/cm, a factor of ten less than that calculated for the Codd and Petch iron. A lower density of grain boundary ledges in a purer material is consistent with Li's analysis of the effect of impurities on the density of grain boundary ledges.

The micrographs of Fig. 11 illustrate the dislocation arrangements near grain boundaries in a sample strained 0.375% at 25°C. Fig. 11a is the arrangement near a boundary away from grain boundary junctions. It is characterized by few dislocation intersections. Fig. 10b shows that near a grain boundary junction there are more dislocations and more interactions due to the stress concentration at the junction. Occasionally a severe tangle can be found emanating from a grain boundary junction or from a region of change in orientation of the boundary, such as in Fig. 12.

C. Formation of Dislocation Tangles and Cell Structure

1. General Features

The change in dislocation density and distribution with increasing strain for iron S-1 is qualitatively similar to the changes in the less pure vacuum-melted iron previously reported (2). In the early stage of deformation the dislocations are generally kinked and nonuniformly distributed; as the amount of strain is increased, the distribution becomes more nonuniform, dislocation tangles are formed and finally a cell structure is developed. This sequence of events for iron S-1 is illustrated in Figs. 13 and 14. The deformation substructure in the higher purity iron is characterized by the more frequent observation of unkinked dislocations in areas removed from tangles, fewer tangles and less severe tangling at small amounts of strain as shown in Fig. 13a. The increased purity of the iron has reduced the tendency for the formation of jogs by reducing the interaction of dislocations with point defects (24), or by reducing the necessity for cross-slip of dislocations (25). The somewhat parallel arrangements of these unjogged dislocations would suggest that cross-slip, the more likely mechanism of jog formation, is reduced. This is probable, since the barriers which necessitate the cross-slip of dislocations are reduced with increased purity. Keh and Weissmann (2) have concluded that tangle formation is the result of interaction of dislocations of a secondary slip system with the jogs formed on primary slip dislocations by the cross-slip mechanism. The observation of fewer and less severe tangles is consistent with a reduction in density of interaction sites, the jogs, and a reduction in the density of grain boundary sources. Tangles may form by direct interaction of slip dislocations of two systems without the requirement of jog formation. In this case, the initial tangle is expected to consist of a rather regular network of dislocations. The arrangement could be a crossed grid (26) or an hexagonal network as observed in molybdenum (27). The hexagonal network arises from the dislocation

reaction

$$\frac{a}{2}[111] + \frac{a}{2}[1\bar{1}\bar{1}] = a[100]$$

Regular networks in individual tangles and cell walls have not been observed frequently in an as-strained vacuum melted iron, but they seem to be a common feature in the higher purity material, as can be seen in Fig. 13a and Fig. 15. The frequency of observation of these fairly regular networks in the tangles and in the cell walls developed from tangles indicates that interaction of dislocations on at least two slip systems is necessary for tangle formation and the development of the cell structure.

The zone axis of the possible crystallographic planes of a cell wall may be determined by means of selected-area diffraction and single-surface trace analysis. The zone axis is that crystallographic direction, in the plane of the foil, which is parallel to the trace of the cell wall in the plane of the foil. With very few exceptions, at least one of the planes of the zone has been of the $\{110\}$, $\{112\}$ or $\{123\}$ type. No other low-index planes have shown such a trend or occurred with the same frequency. This result strongly suggests that the plane of the cell wall in iron is then $\{110\}$, $\{112\}$ or $\{123\}$. The development of cell walls on these planes could be the result of the interaction of the dislocations of two slip systems to form the initial tangles on these planes or the result of cooperative motion of the tangles leading to alignment in the slip planes (2,28).

The development of deformation substructure in iron B-13 is similar to that in iron S-1. Lesser amounts of strain to produce a comparable structure were required since the grain size of B-13 was smaller.

The ten-pass zone-refined iron B-3 has presented two serious experimental difficulties which hinder study of this material by electron transmission microscopy. The production of usable thin foils has been sporadic and their preparation has required precise control of composition of polishing solution and polishing conditions. The more serious difficulty has been a decrease in the density of dislocations and an almost certain rearrangement as a result of the thinning operation. An excessive amount of dislocation motion, not typical of less pure iron, has been noted during examination of foils in the microscope. Fig. 16 is an illustration of the degree of movement of dislocations in foils of iron B-3. The variation of dislocation density and distribution in this iron is considerably more than normally encountered in this type of study. Irons S-1 and B-13 did not show such a large variation and the structures observed in these irons can be considered "typical". The inconsistency of the deformation substructure in a foil of B-3, as shown in Fig. 17, makes it difficult to define any single structure as typical of this material. For the purpose of discussion, the typical unaltered structure of this iron after deformation will be considered as that structure with the greatest dislocation density, the most severe tangles and the best developed cell structure. The change in deformation substructure with increasing strain for iron B-3 is shown in Figs. 18 and 19. A significant degree of tangling

and cell formation is accomplished only after about 5% strain at room temperature. An appreciable change in the flow stress at -78°C, after prestrain at room temperature, would not be expected for prestrains less than about 5%, in agreement with the tensile test results given in Fig. 3. Comparison with the structures of iron S-1, in Figs. 13 and 14, indicates that the distribution of dislocations is more uniform and the cell structure not as well developed in iron B-3. The limiting cell size for the vacuum-melted iron was 1.5μ whereas in this investigation the limiting cell size increases somewhat with increasing purity from 2μ for S-1 and B-13 to about 2.5μ for B-3. As the purity increases, the density of grain boundary ledge sources decreases and the necessity for cross-slip decreases. A decrease in these two factors leads necessarily to a decreased dislocation density, fewer and less severe tangles, and consequently a larger cell structure with a more regular distribution of dislocations within the cell walls. Dynamic recovery at room temperature in the purer irons could also result in a larger cell size with cell walls of somewhat regular networks of dislocations.

2. Effect of Deformation Temperature on the Dislocation Distribution

As previously reported (2), the tendency for cell formation becomes less and the dislocation distribution becomes more uniform for a given strain as the temperature of deformation is decreased. The dislocation structures of iron S-1 deformed at 25 and -78°C to about the same strain are shown in Fig. 20. The dislocation distribution at -78°C is considerably more uniform and the dislocations are more uniformly kinked than at 25°C. This structure has been explained on the basis of more frequent cross slip, but over smaller distances than at room temperature (2). Figs. 21 and 22 illustrate that the same temperature effect on the distribution of dislocations is present in iron B-3. In this iron, however, the dislocations formed by low temperature deformation do not appear to be severely kinked as in iron S-1, nor as uniformly distributed, and occurrence of loose tangles is also more frequent. These observations are consistent with dislocation movement, resulting from the thinning operation. Such movement could cause a decrease in the density of jogs on the dislocations and rearrangement of a uniform distribution to a less uniform distribution.

The dislocation structures developed in iron B-3 by deformation at -196°C are shown in Fig. 23. The distribution is much more uniform consisting of at least two sets of parallel dislocations; tangles are not formed up to the point of fracture of this iron at about 14% strain. The curvatures at dislocation intersections, such as shown in Fig. 24, suggest that possibly three slip systems were active in this particular grain. Two of the sets of dislocations have the same Burgers vector and at the point of intersection there is mutual annihilation and a rounding off of the intersection point, as indicated in area A in Fig. 24. The third set of parallel dislocations has a different Burgers vector, such that there is interaction to form an a[100] segment at the point of intersection. In this case, the sharp points of the dislocation interaction remain, and examination of Fig. 24 reveals that the a [100] segments have two directions as is expected. This interaction is noted at points B and C in Fig. 24.

3. Effect of Strain Rate on the Dislocation Distribution

The effect of increasing the strain rate of deformation is analogous to decreasing the temperature of deformation, that is, the tendency for cell formation becomes less pronounced and the dislocation distribution becomes more uniform for a given strain as the strain rate is increased. The degree of change in dislocation distribution with a change in strain rate is not as marked as for a change in temperature. Differences are most apparent at small amounts of deformation and for changes in strain rate of several orders of magnitude. Fig. 25 illustrates the difference in dislocation distribution in iron S-1 strained 2.5% at strain rates of 2.5×10^{-5} sec^{-1} and 1.25×10^{-2} sec^{-1}. These structures may also be compared with that shown in Fig. 13a. The dynamic theory of yielding proposed by Johnston and Gilman (29) requires either an increase in the number of mobile dislocations or an increase in the average velocity of dislocations to accommodate an increase in strain rate. The more uniform distribution of dislocations could be accomplished by an increase in the amount of cross-slip to increase the number of mobile dislocations or an increase in the velocity of the edge components of dislocations relative to the velocity of the screw components. The latter would result in mainly screw dislocations being left in the structure. Since the densities of dislocations are not very different, as is also the case for low temperature deformation (2), it may be assumed that the uniform distribution is more likely the result of an increase in the velocity of edge dislocations.

As the amount of strain is increased the differences due to strain rate become less apparent and a well developed cell structure is formed.

4. Effects of Alloying on Dislocation Distribution

The influence of alloy additions on the dislocation arrangements in iron has not received much study except for iron-silicon (30), iron-phosphorus (20), and iron-manganese (5) alloys. In the first two cases the effect of alloy addition was to decrease the tendency for cell formation and to produce a more uniform distribution of dislocations. The effect is analogous to lowering the temperature or increasing the strain rate of deformation. It is well known that silicon and phosphorus are very pronounced solid-solution strengtheners and substantially increase the tendency for mechanical twinning. Manganese is not nearly as potent a solid-solution strengthener and has been reported (5) to result in a less uniform distribution of dislocations and to increase the tendency for cell formation at room temperature, as shown in Fig. 26. An increase in alloy content would result in an increase in grain boundary sources thus leading to increased dislocation density and enhanced cell formation. The differences in dislocation distribution for different alloy additions cannot be explained solely on changes on the density of grain boundary sources. In the case of silicon or phosphorus additions the random distribution has been attributed to a decreased mobility of the dislocations and, in particular, a greater decrease in the mobility of screw components. The decrease could be the result of an increased frictional stress or an increase in the density of vacancies which might interact with the screw dislocations to form jogs. The addition of

0.6 wt.% manganese apparently does not markedly influence the relative mobilities of the edge and screw dislocations and therefore the distribution of dislocations does not tend to be random. The effect of manganese, therefore, is primarily to increase the average density for a given strain by increasing the density of grain boundary sources. The binding effect of manganese on these sources is small since the difference in yield stress of pure iron and iron-0.6 wt.% manganese is not large (5).

The increased tendency for retention of a nonuniform distribution and the formation of tangles and cell walls in the manganese alloy is also observed at lower temperatures or increased strain rates. This may be seen by comparison of Fig. 27a with Fig. 20b and Fig. 27b with Fig. 25b.

4. Summary

1. The development of deformation substructure in zone-refined iron is similar to that reported for vacuum-melted iron and other body-centered cubic metals.

2. The primary effect of increased purity is to decrease the density of grain boundary sources and to decrease the necessity for cross-slip. This results in fewer and less severe tangles of dislocations and a small increase in the size of cells.

3. The cell walls in the purer iron consist of somewhat regular networks of dislocations, as do the initial tangles.

4. In a very high-purity iron the dislocation density may decrease and the dislocations may change their distribution as a result of the thinning process.

5. A decrease in the temperature of deformation or an increase in the strain rate decreases the tendency for cell formation and produces a more uniform distribution of dislocations.

6. The addition of an alloying element which is not a strong solid-solution strengthener increases the dislocation density and tendency for cell formation primarily by increasing the density of grain boundary sources.

Acknowledgment

The authors wish to thank J. C. Raley and R. D. Schoone for their assistance in this investigation. The zone-refined materials prepared by Battelle Memorial Institute under the sponsorship of the American Iron and Steel Institute were obtained through the courtesy of J. W. Halley. The ten-pass zone-refined iron was prepared by B. F. Oliver of the E. C. Bain Laboratory, U. S. Steel Corporation. We are indebted to A. S. Keh and J. C. M. Li, also of this Laboratory, for helpful discussions.

References

1. A. S. Keh, Direct Observations of Imperfections in Crystals, Interscience, New York, 1962, 213.

2. A. S. Keh and S. Weissmann, to be published.

3. W. S. Owen, this symposium, paper 9.

4. A. Berghezan, this symposium, paper 17.

5. W. C. Leslie, J. T. Michalak and F. W. Aul, to be published, Iron and Its Dilute Solid Solutions, Interscience.

6. H. Hu, to be published, Recovery and Recrystallization of Metals, Interscience.

7. J. L. Walter, this symposium, paper 8.

8. W. C. Leslie and A. S. Keh, J. Iron Steel Inst. 200, 722 (1962).

9. A. R. Rosenfield and W. S. Owen, this symposium, paper 14.

10. A. S. Keh, W. C. Leslie and G. R. Speich, this symposium, paper 16.

11. W. C. Leslie, F. J. Plecity and J. T. Michalak, Trans. AIME 221, 691 (1961).

12. W. C. Leslie, F. J. Plecity and F. W. Aul, Trans. AIME 221, 982 (1961).

13. E. P. Abrahamson, II and B. S. Blakeney, Jr., Trans. AIME 218, 1101 (1960).

14. J. J. Cox, G. T. Horne and R. F. Mehl, Trans. ASM 49, 118 (1957).

15. J. S. Erickson, J. Appl. Phys. 33, 2499 (1962).

16. J. S. Koehler, Phys. Rev. 86, 52 (1952).

17. J. R. Low, Jr. and R. W. Guard, Acta Met. 7, 171 (1959).

18. W. C. Leslie, Acta Met. 9, 1004 (1961).

19. J. C. M. Li, to be published, Trans. AIME.

20. E. Hornbogen, to be published, Trans. ASM.

21. S. Weissmann, Trans. ASM 52, 599 (1960).

22. E. O. Hall, Proc. Phys. Soc. B64, 747 (1951).

23. I. Codd and N. J. Petch, Phil. Mag. 5, 30 (1960).

24. J. T. Fourie and H. G. T. Wilsdorf, J. Appl. Phys. 31, 2219 (1960).

25. W. G. Johnston and J. J. Gilman, J. Appl. Phys. 31, 632 (1960).

26. J. C. M. Li, J. Appl. Phys. 32, 1873 (1961).

27. R. Benson, G. Thomas, and J. Washburn, Direct Observation of Imperfections in Crystals, Interscience, New York, 1962, 375.

28. J. C. M. Li, Direct Observation of Imperfections in Crystals, Interscience, New York, 1962, 234.

29. W. G. Johnston and J. J. Gilman, J. Appl. Phys. 30, 129 (1959).

30. J. R. Low, Jr. and A. M. Turkalo, Acta Met. 10, 215 (1962).

Table I

High-Purity Materials Investigated

Material	Designation	Method of Purification	Grain Size
Fe*	S-1	Zone-melted in horizontal boat. Two passes.	90μ
Fe*	B-13	Zone-refined by floating-zone technique. One pass.	43μ
Fe**	B-3	Zone-refined by floating-zone technique. Ten passes.	42μ
Fe-0.60 Mn*	S-8	Zone-melted in horizontal boat. One pass.	60μ

* Supplied by Battelle Memorial Institute.

** Supplied by B. F. Oliver, United States Steel Corporation.

Table II

Nonmetallic Impurity Contents, PPM

Material	C	N	H	O
S-1	15	6	0.2	25
B-13	10	<0.05	0.9	1.2
B-3	15	5	<1	<5
S-8	15	6	0.4	25

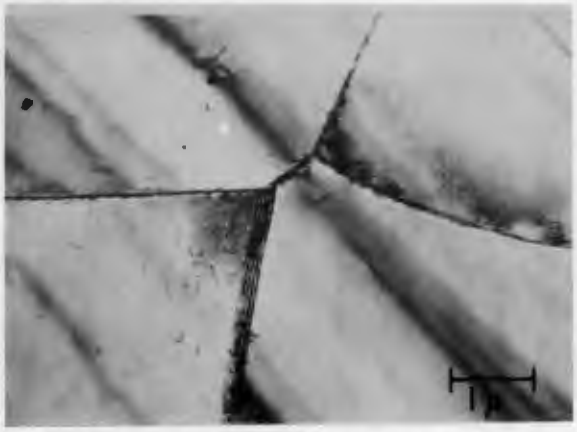

(a) INITIAL, RECRYSTALLIZED

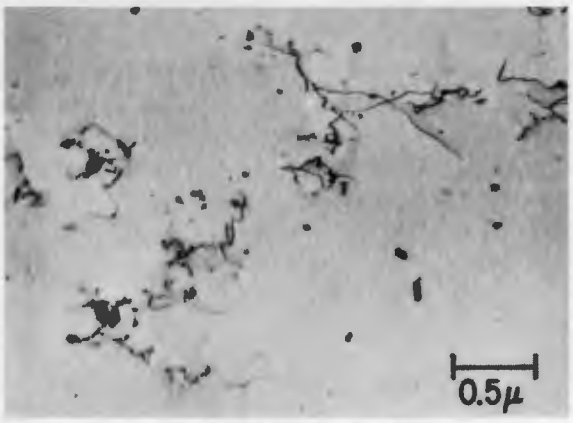

(b) 1 % STRAIN

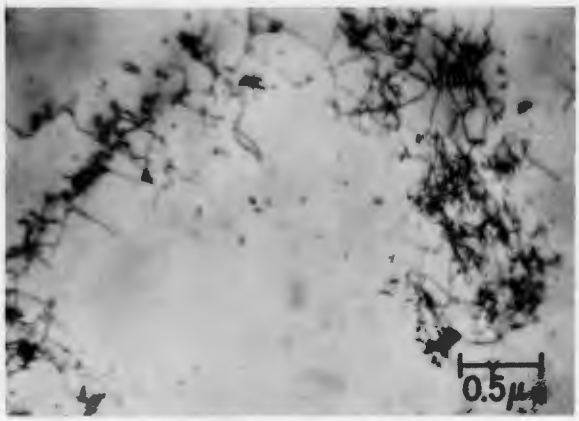

(c) 3 1/2 % STRAIN

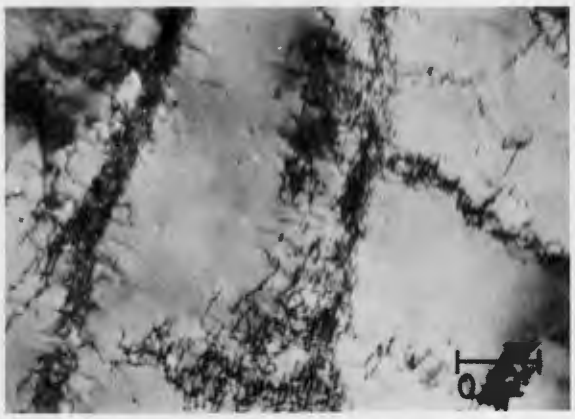

(d) 9 % STRAIN

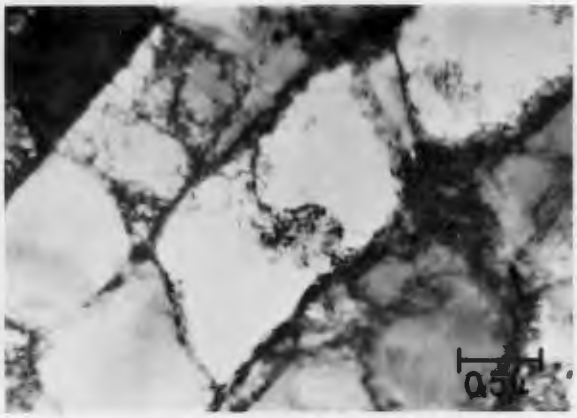

(e) 20 % STRAIN

FIG. 1 -- DEVELOPMENT OF DEFORMATION SUBSTRUCTURE IN IRON. (See ref. 2).

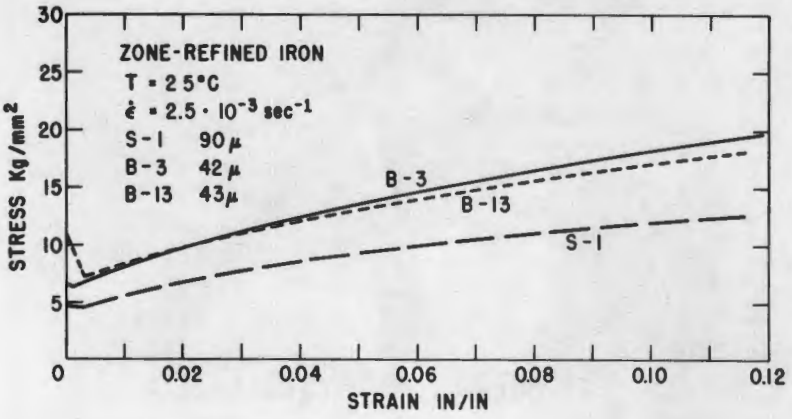

FIG. 2 -- STRESS-STRAIN CURVES FOR POLYCRYSTALLINE HIGH-PURITY IRON DEFORMED AT 25°C.

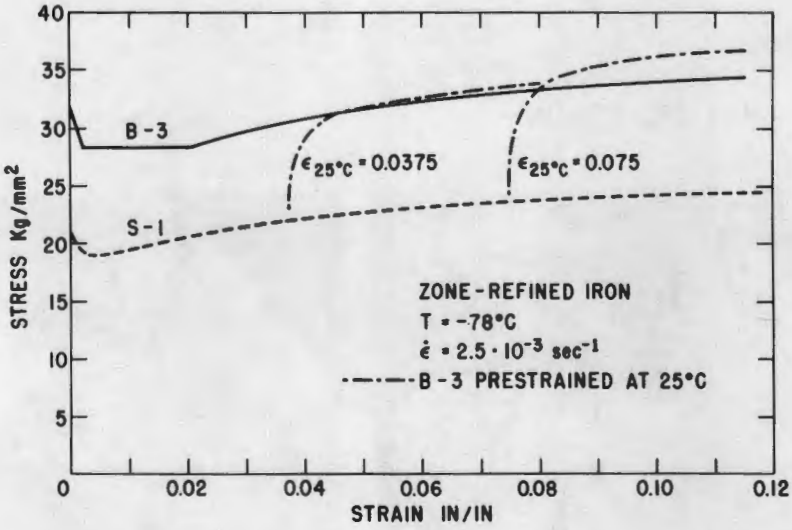

FIG. 3 -- STRESS-STRAIN CURVES FOR POLYCRYSTALLINE HIGH-PURITY IRON DEFORMED AT -78°C.

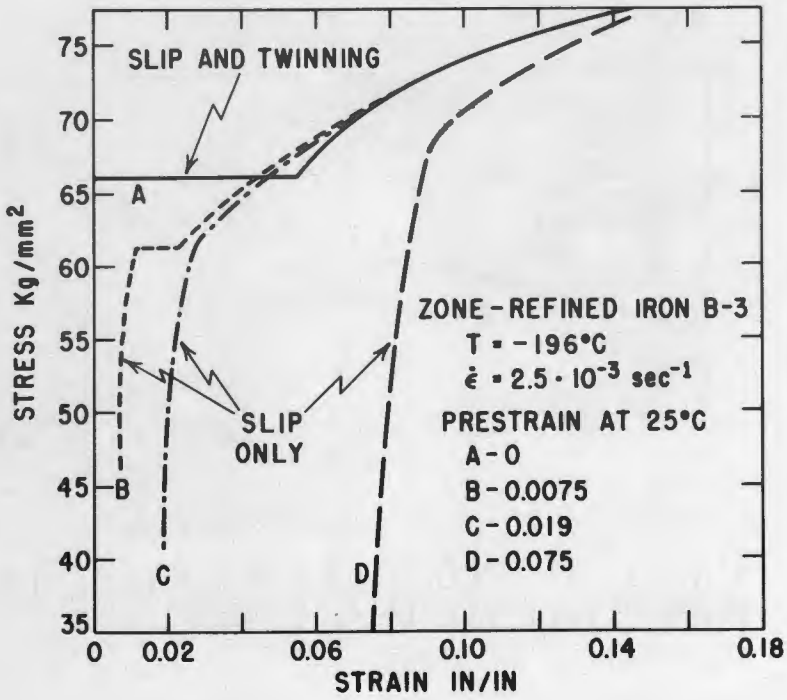

FIG. 4 -- STRESS-STRAIN CURVES FOR POLYCRYSTALLINE HIGH-PURITY IRON DEFORMED AT -196°C.

FIG. 5 -- LUDERS FRONT IN IRON B-3 STRAINED AT -196°C. 100X. UNETCHED SURFACE.

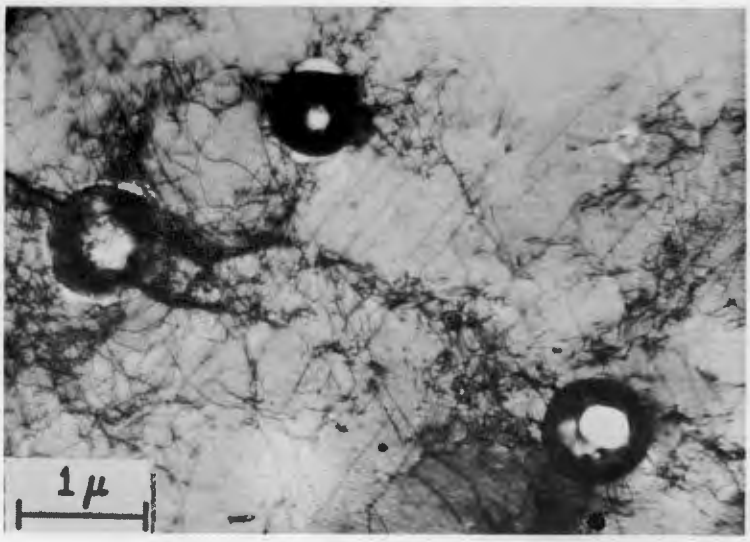

FIG. 6 -- WELL-DEVELOPED CELLS AROUND LARGE PRECIPITATED PARTICLES. Fe-0.015% Bi, C. R. 10%, LONGITUDINAL SECTION. (See ref. 5).

FIG. 7 -- DISLOCATIONS ORIGINATING AT A GRAIN BOUNDARY. Fe-1.78 wt. % P, 1.0% STRAIN. (See ref. 20).

FIG. 8 -- STRUCTURE OF RECRYSTALLIZED GRAINS IN IRON.

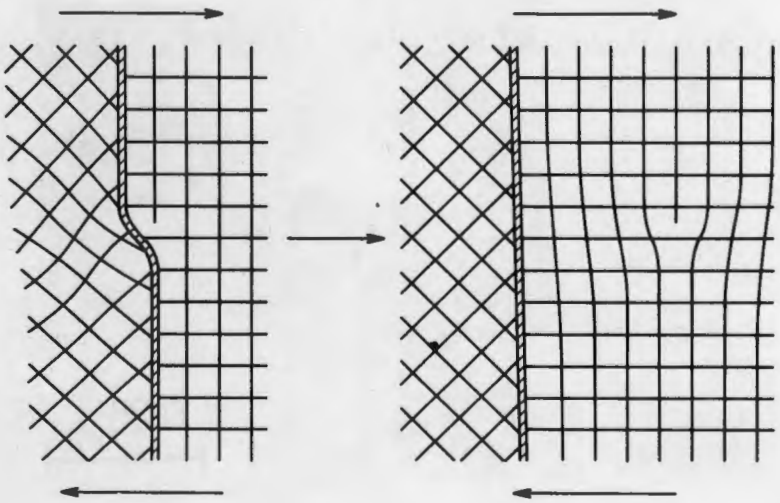

FIG. 9 -- GRAIN BOUNDARY LEDGE ACTING AS DONOR OF DISLOCATION. (See ref. 19).

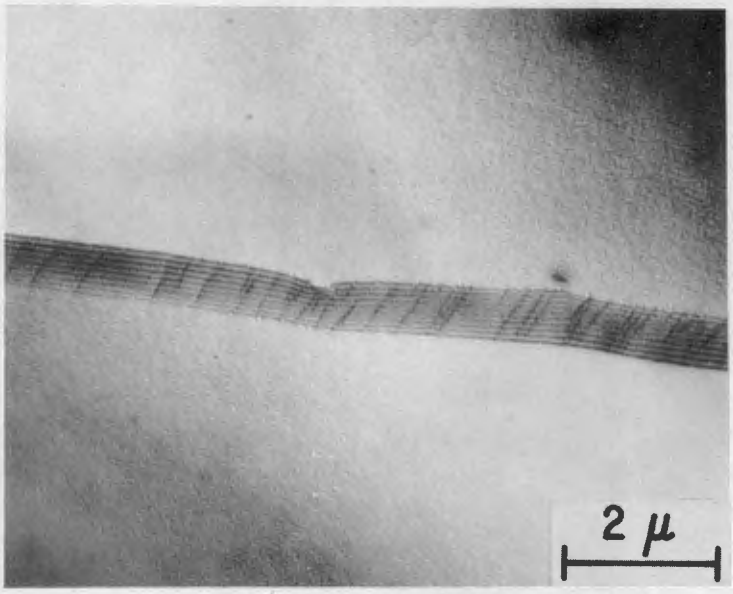

FIG. 10 -- GRAIN BOUNDARY LEDGES IN RECRYSTALLIZED IRON.

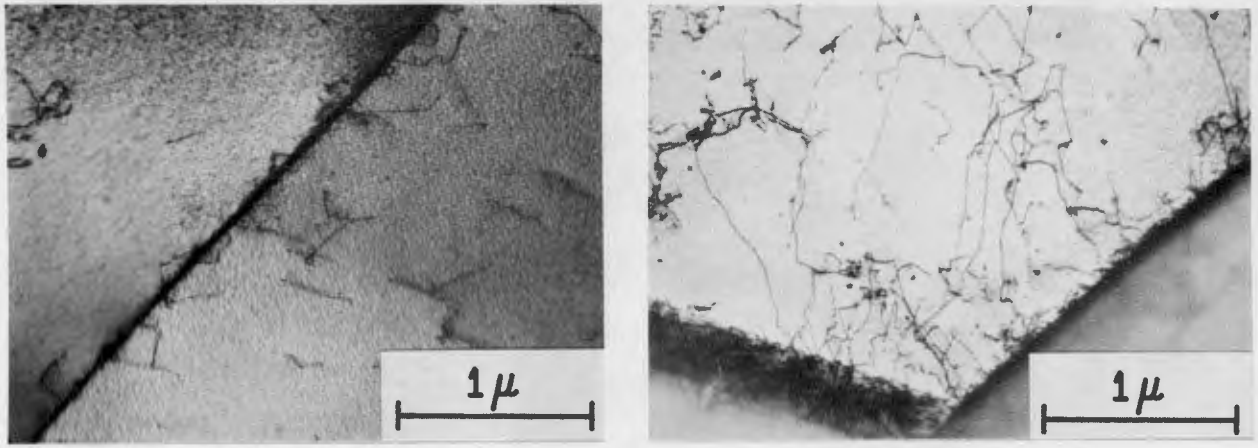

(a) (b)

FIG. 11 -- DISLOCATION ARRANGEMENTS IN IRON STRAINED 0.375% AT 25°C, (a) AT GRAIN BOUNDARY, (b) AT GRAIN BOUNDARY JUNCTION.

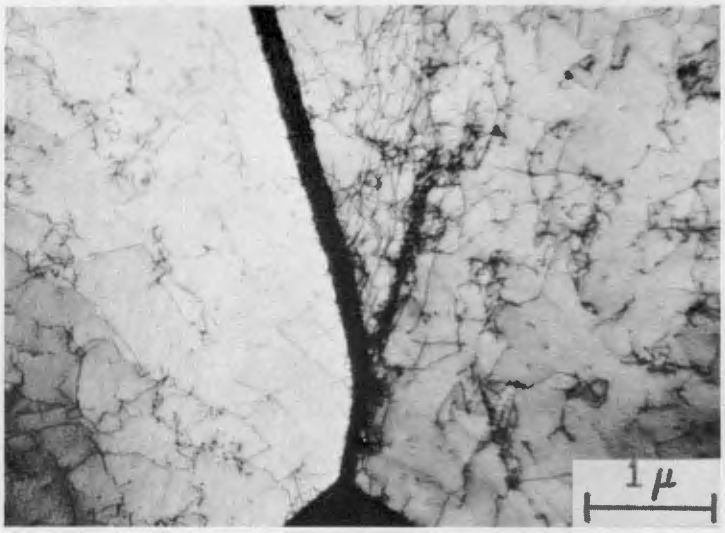

FIG. 12 -- DISLOCATION TANGLE INITIATED FROM A GRAIN BOUNDARY KINK.

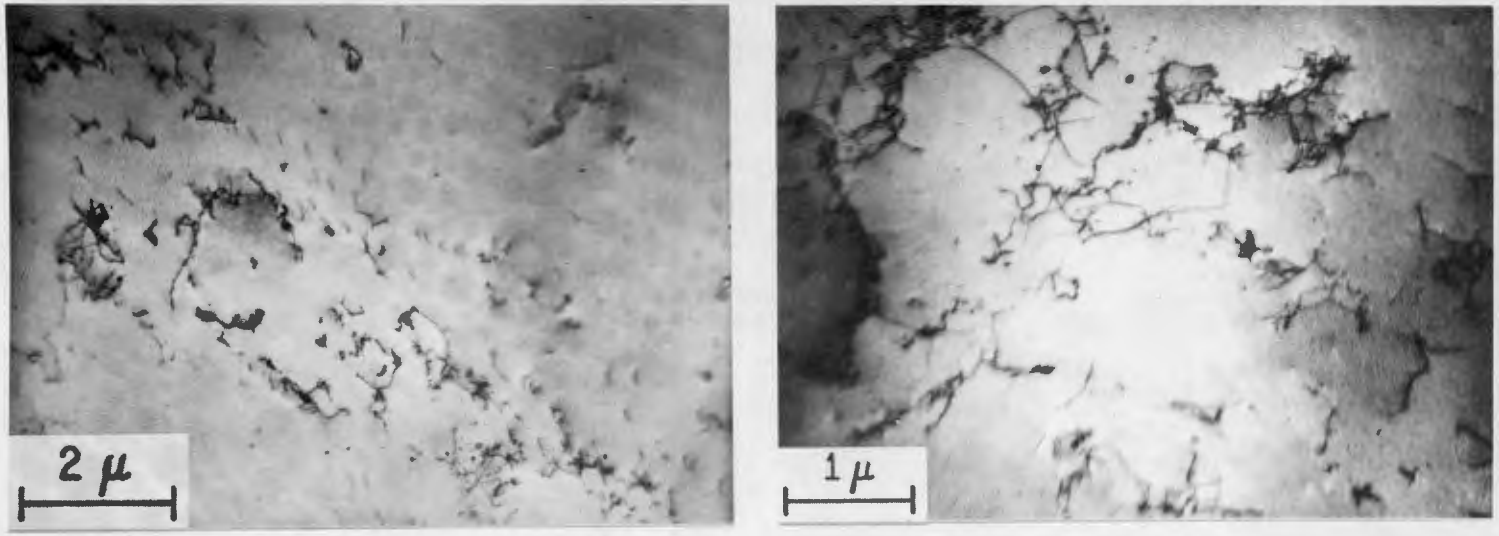

(a) (b)

FIG. 13 -- DISLOCATION STRUCTURE IN IRON S-1 STRAINED AT 25°C. (a) 2.5% STRAIN, (b) 4% STRAIN.

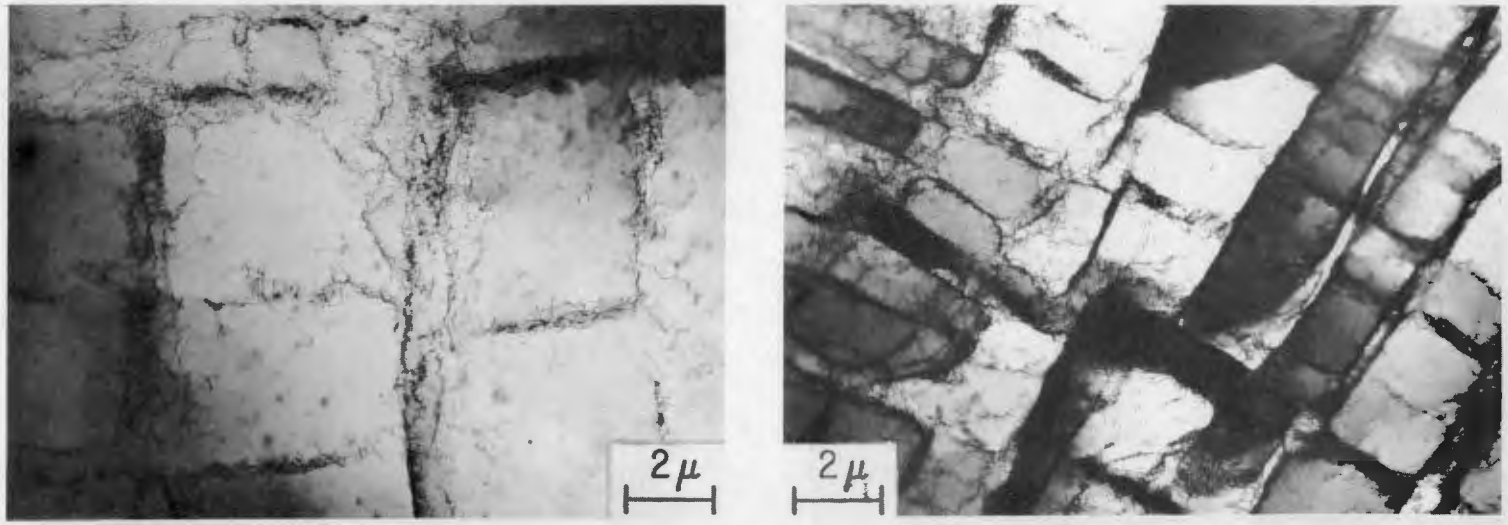

(a) (b)

FIG. 14 -- DISLOCATION STRUCTURE IN IRON S-1 STRAINED AT 25°C. (a) 7.0% STRAIN, (b) 15% STRAIN.

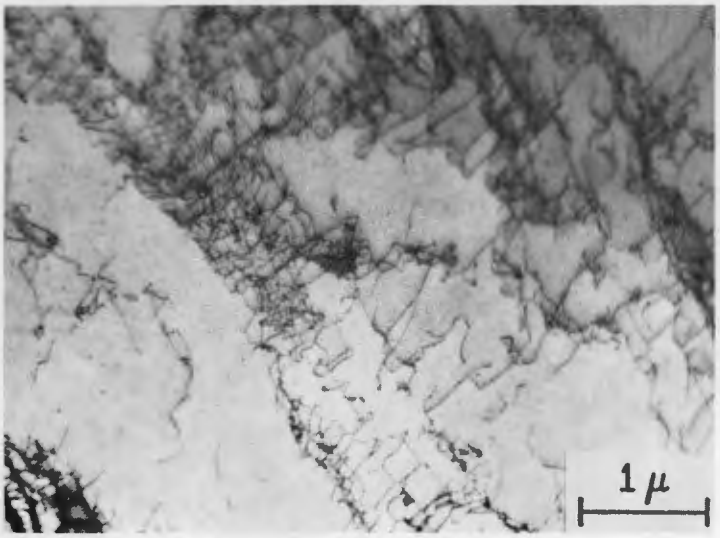

FIG. 15 -- REGULAR NETWORKS OF DISLOCATIONS IN CELL WALLS OF IRON.

FIG. 16 -- TRAILS OF MOVING DISLOCATIONS IN IRON B-3.

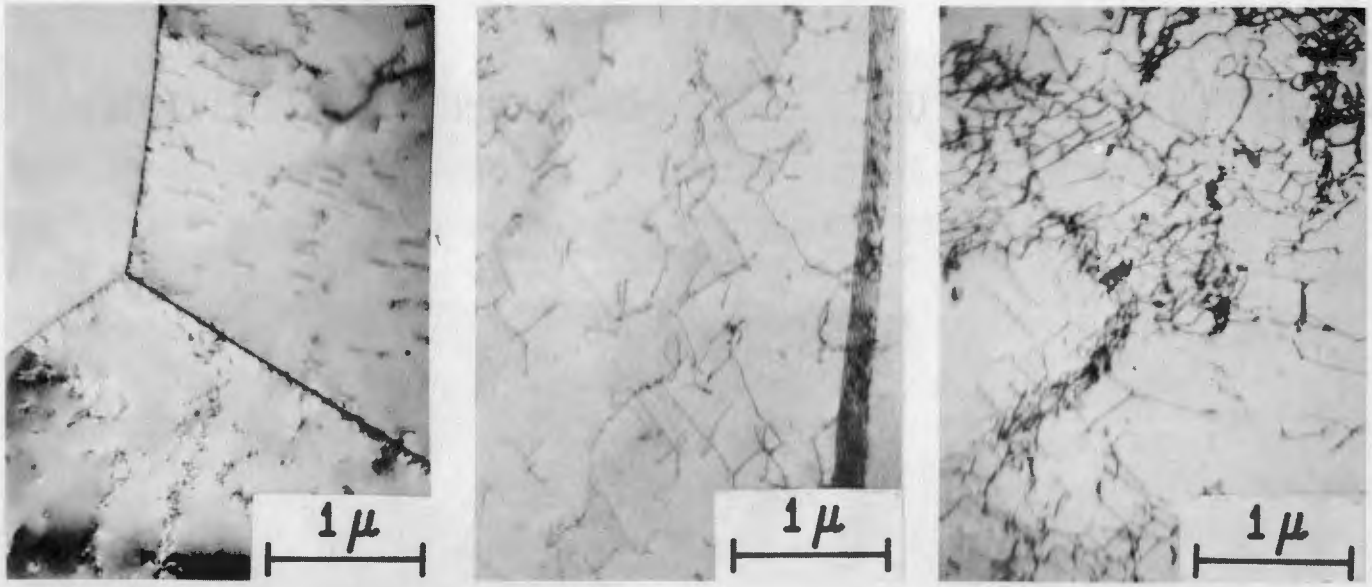

FIG. 17 -- VARIATION OF DISLOCATION STRUCTURE IN IRON B-3 AFTER 5.5% STRAIN AT 25°C.

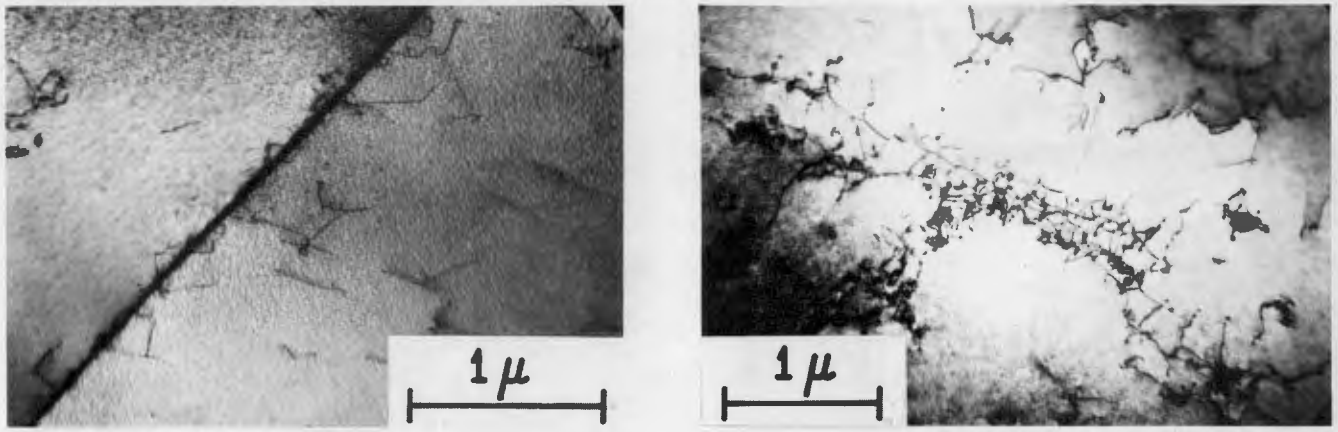

(a) (b)

FIG. 18 -- DISLOCATION STRUCTURE IN IRON B-3 STRAINED AT 25°C. (a) 0.375% STRAIN, (b) 2.5% STRAIN.

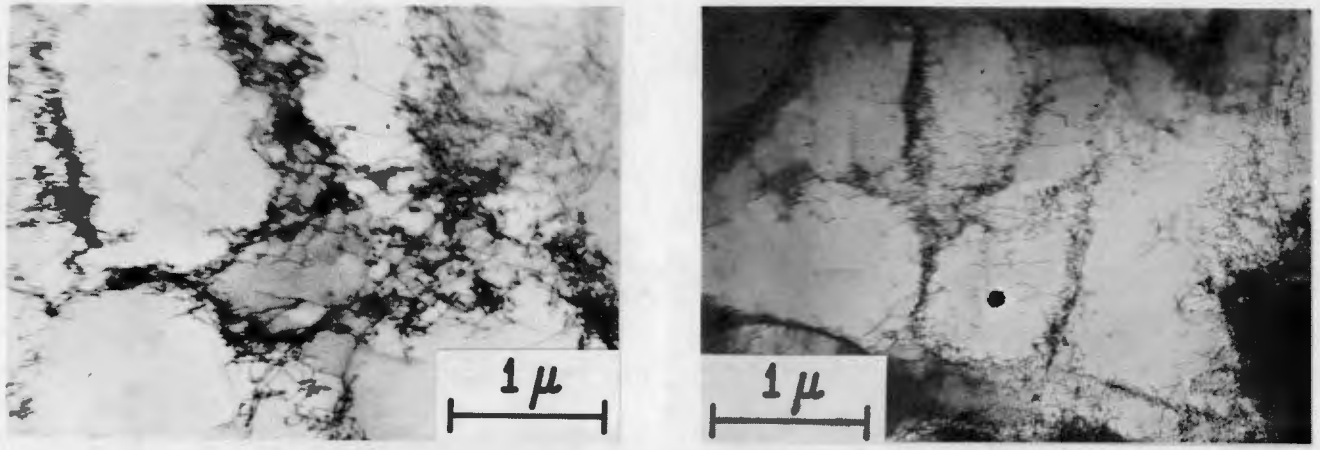

(a) (b)

FIG. 19 -- DISLOCATION STRUCTURE IN IRON B-3 STRAINED AT 25°C. (a) 5.5% STRAIN, (b) 15.5% STRAIN.

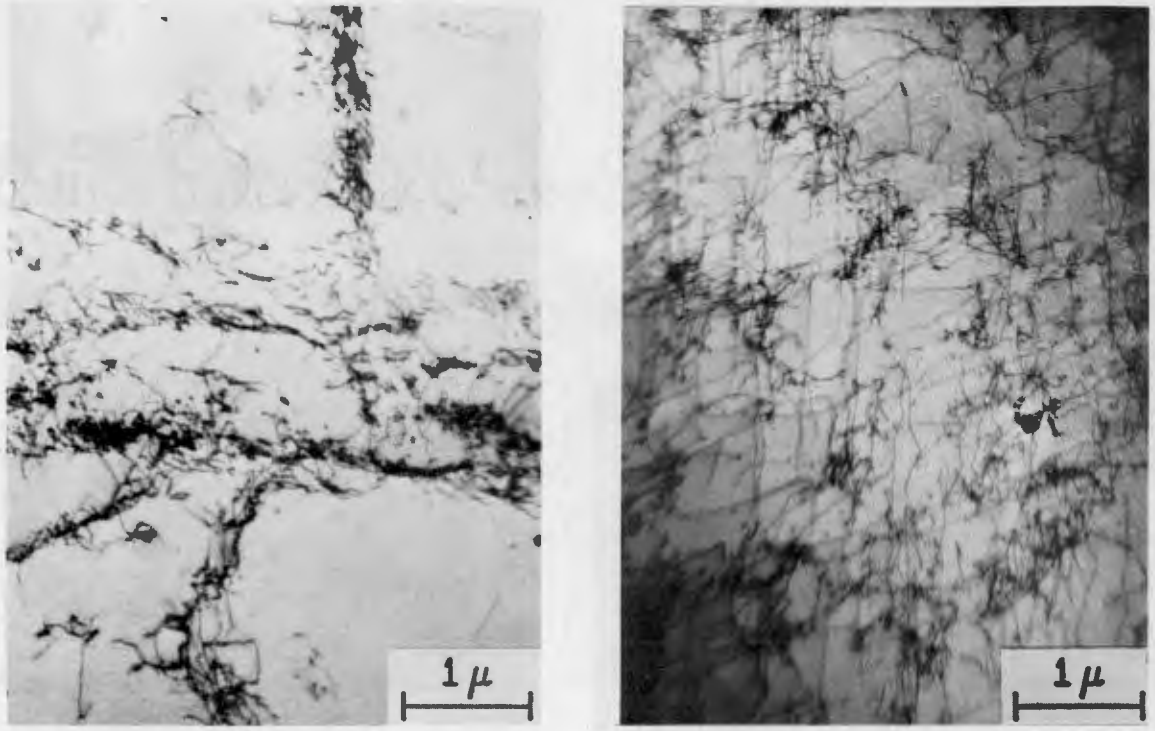

(a) (b)

FIG. 20 -- DISLOCATION STRUCTURE IN IRON S-I STRAINED 7.0% AT (a) 25°C AND (b) -78°C.

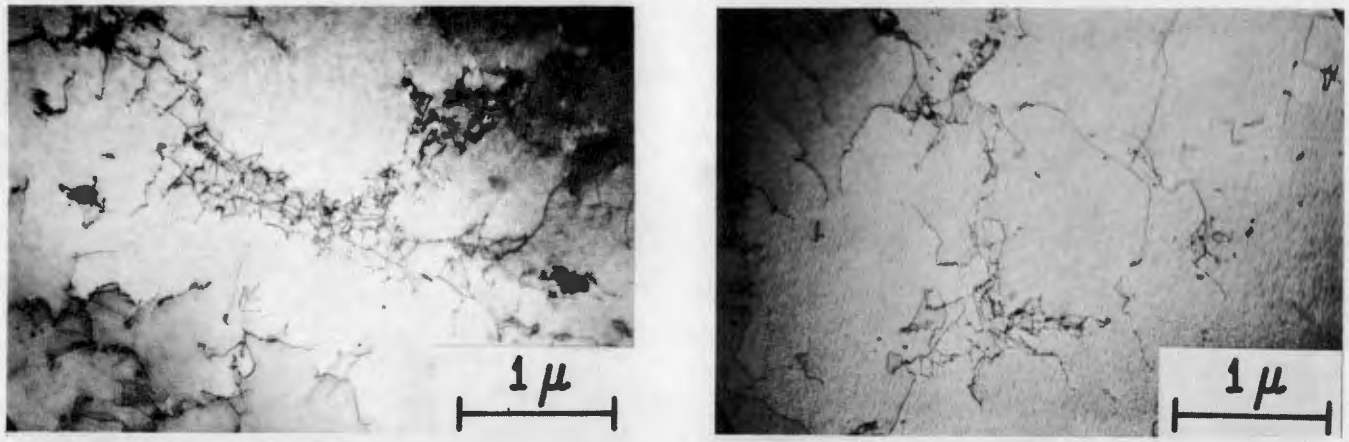

(a) (b)

FIG. 21 -- DISLOCATION STRUCTURE IN IRON B-3 STRAINED 2.5% AT (a) 25°C AND (b) -78°C.

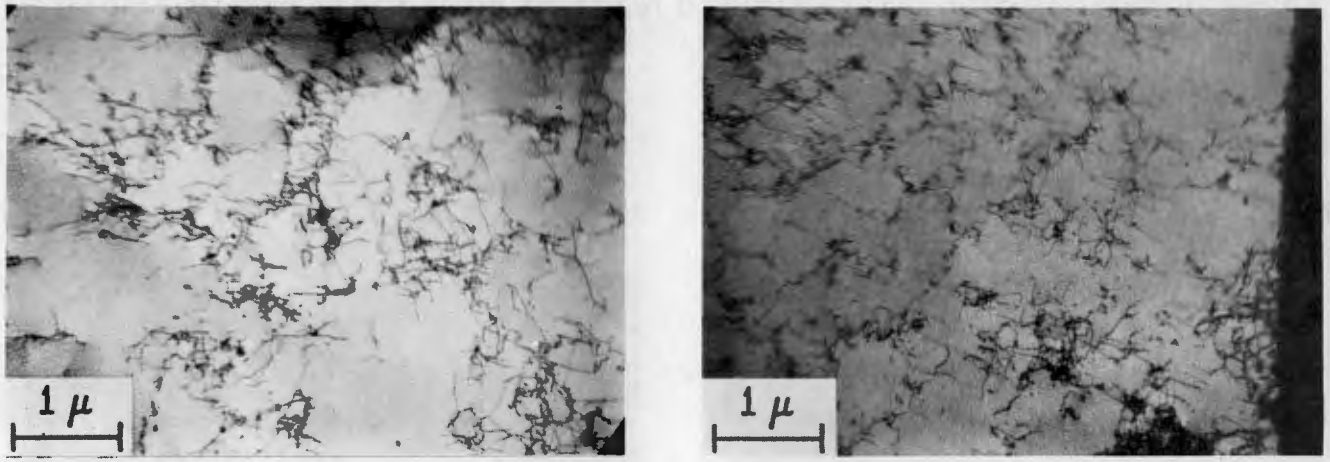

(a) (b)

FIG. 22 -- DISLOCATION STRUCTURE IN IRON B-3 STRAINED 5.5% AT (a) 25°C AND (b) -78°C.

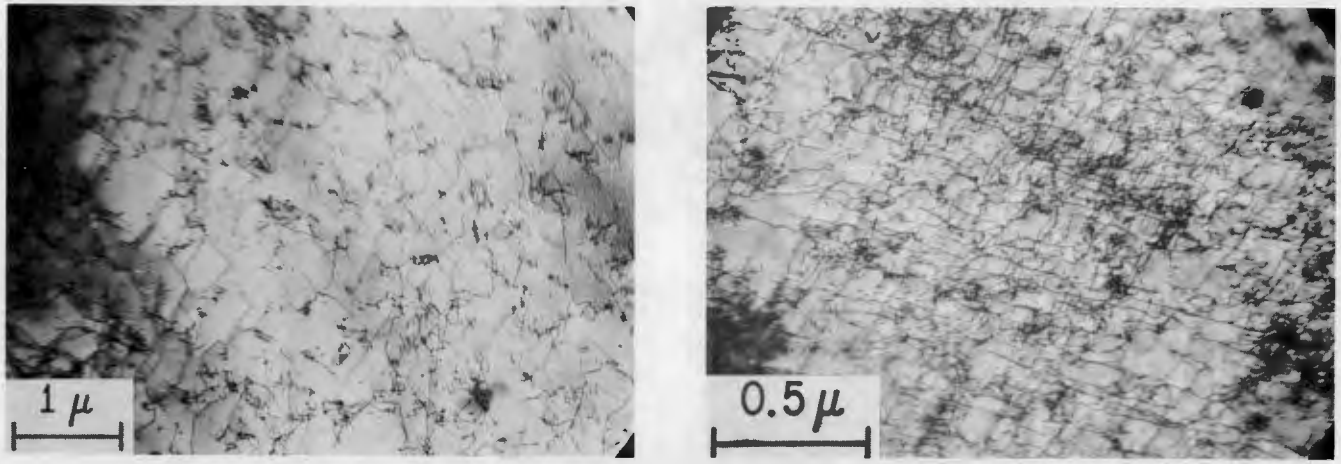

(a) (b)

FIG. 23 -- DISLOCATION STRUCTURE IN IRON B-3 STRAINED AT -196°C. (a) 5.5% STRAIN, (b) 14.0% STRAIN.

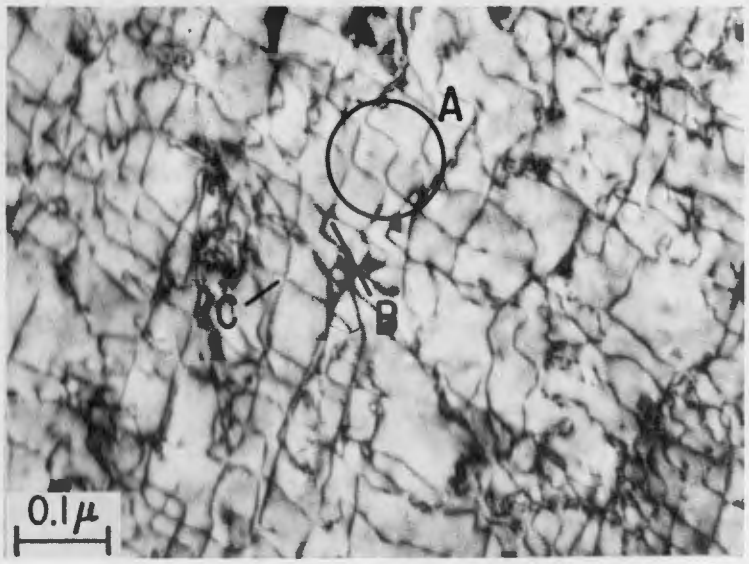

FIG. 24 -- DISLOCATION INTERACTIONS IN IRON B-3 STRAINED 14.0% AT -196°C.

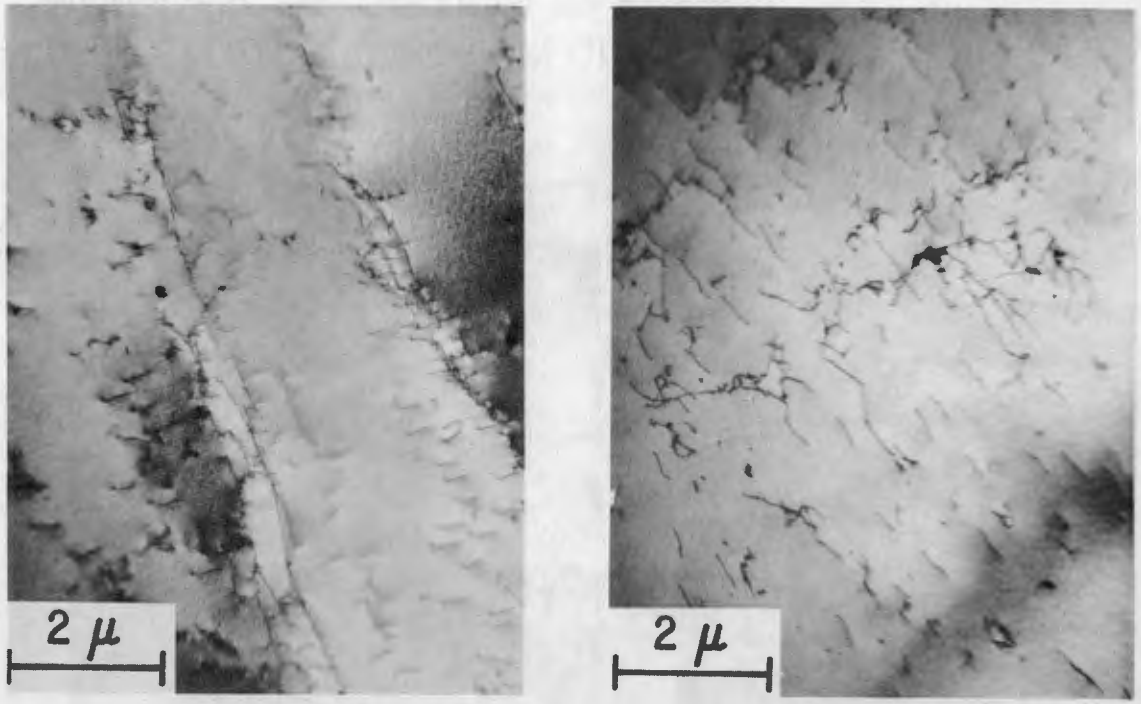

FIG. 25 -- DISLOCATION STRUCTURE IN IRON S-1 STRAINED 2.5% AT 25°C AT STRAIN RATES OF (a) 2.5×10^{-5} sec^{-1} AND (b) 1.25×10^{-2} sec^{-1}.

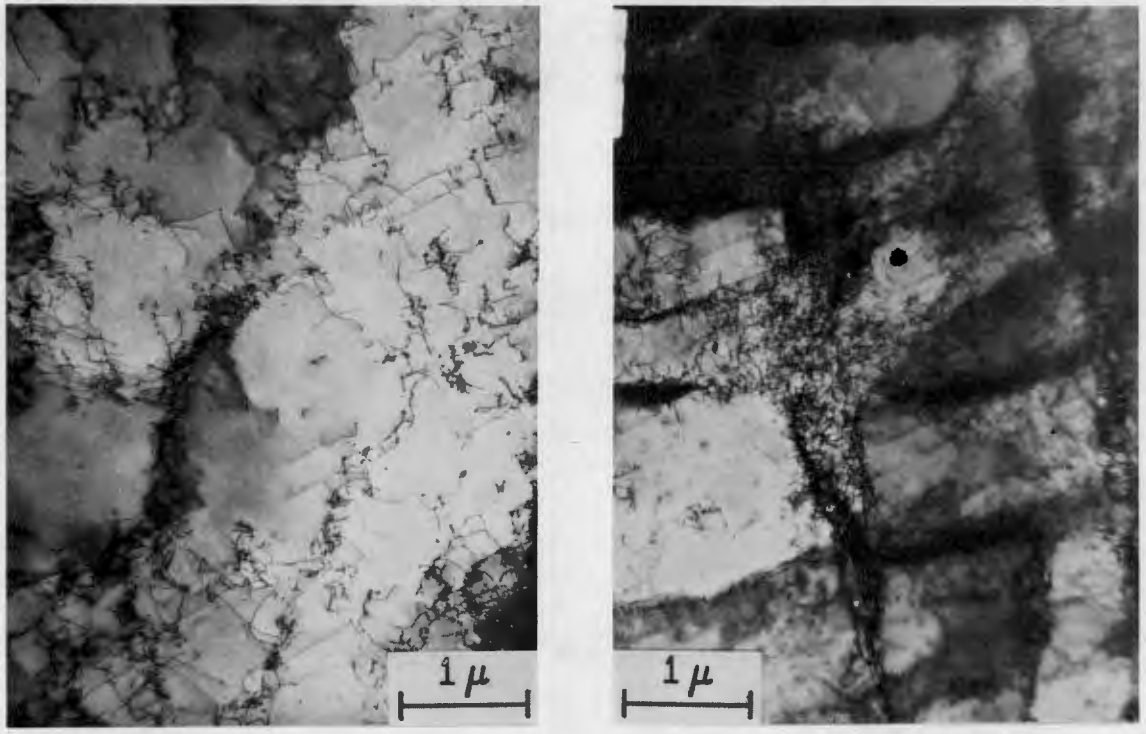

(a) (b)

FIG. 26 -- DISLOCATION STRUCTURE IN (a) IRON S-I, AND (b) IRON-0.60 wt. % MANGANESE S-8, STRAINED 15% AT 25°C.

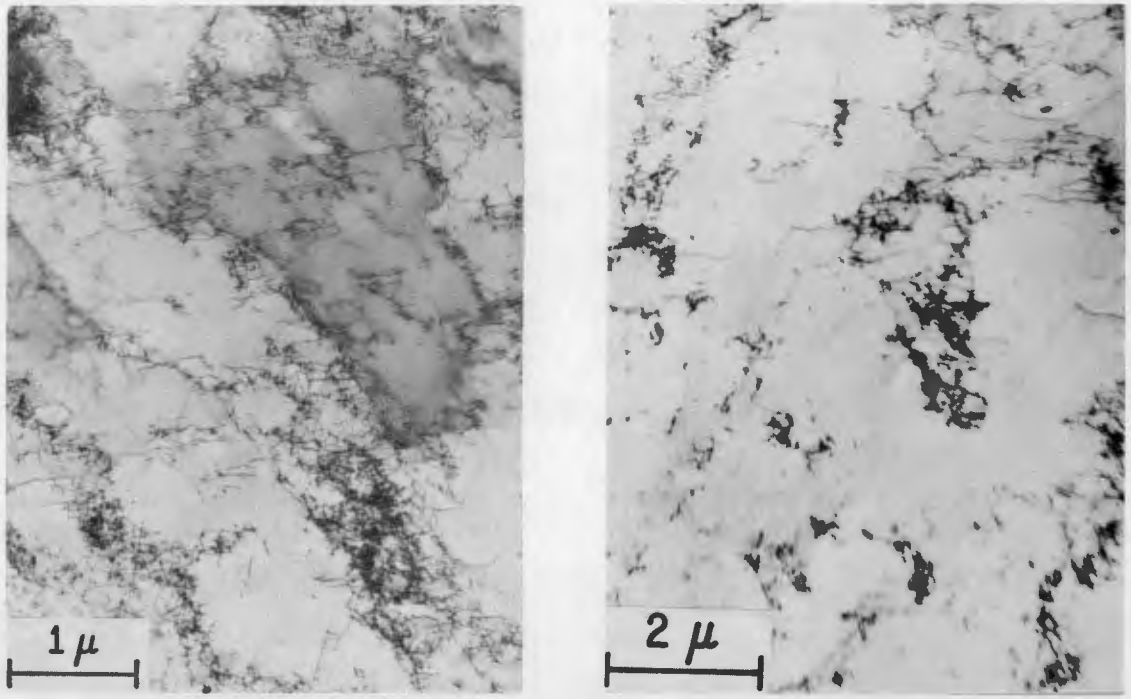

FIG. 27 -- DISLOCATION STRUCTURE IN IRON-0.60 wt. % MANGANESE. (a) 9.5% STRAIN AT -78°C, (b) 2.5% STRAIN AT 25°C AND STRAIN RATE OF 1.25×10^{-2} sec^{-1}.